Effects of surface affinity on the ordering dynamics of self-assembled monolayers of chain molecules: Transition from a parallel to a perpendicular structure

Toshiaki Miura and Kazuhiko Seki

National Institute of Advanced Industrial Science and Technology (AIST), AIST Central2, 1-1 Umezono, Tsukuba, Ibaraki 305-8568, Japan

(Received 10 September 2014; revised manuscript received 16 February 2015; published 19 May 2015)

The effects of surface interactions on the ordering dynamics of self-assembled monolayers (SAM) of chain molecules were studied using molecular dynamics simulations. When the strength of surface–chain interactions was equal to or less than that of chain–chain interactions, domains of chain molecules adsorbed perpendicular to the surface ("upright" chains) formed on the surface. Although chain molecules adsorbed parallel to the surface ("lying" chains) were initially observed on the surface, they did not develop into two-dimensionally aligned structures. In contrast, when the strength of surface–chain interactions was at least twice that of chain–chain interactions, the proportion of upright chain molecules was initially small, and the reorientation of lying chains was observed shortly afterwards. In this case, the reorientation from lying to upright configuration developed slowly from the domain boundaries of two-dimensionally aligned structures late in the calculation period. Although the orientation processes of chain molecules on surfaces were strongly influenced by the strength of surface–chain interactions, the total adsorption rate on the surface was not. We also analyzed the maximum area of domains formed by lying chains. The development of two-dimensionally aligned domains required strong surface–chain interactions to prevent the spontaneous formation of nuclei of upright domains.

DOI: 10.1103/PhysRevE.91.052604 PACS number(s): 82.35.−x, 68.08.−p

I. INTRODUCTION

Structures of chain molecules on surfaces are formed through complicated ordering processes, and the alignment of molecules at interfaces is an important factor that controls their functionality and tribology. Some kinds of chain molecules, such as alkanethiols, form self-assembled monolayers (SAMs), in which the chain molecules in solution spontaneously form aligned monolayer structures on a substrate [1]. There have been many experimental studies on the formation of SAMs [2–7]. The ordering process of chain-like molecules involves two steps, rapid adsorption and slow chain ordering. However, the ordering dynamics of chain molecules are less explored than the static properties of chain molecules in equilibrium states, partly because it is difficult to observe ordering processes directly at the microscopic level. For example, the observation of ordering of chain molecules by scanning tunneling microscopy has suggested that a two-dimensional pattern of chain molecules forms under certain conditions [8–11], but it is still unclear whether these striped patterns form in various molecules or solutions.

Observation of the dynamics of chain molecules by computer simulation is also challenging. Compared to the simulation of the various equilibrium properties of chain molecules in the vicinity of a surface [12–31], studies on dynamical behavior require more computational resources. Further simulation studies on dynamics would be useful to understand the detailed order formation mechanism [32–36].

Recently, we studied the ordering processes of SAMs of chain molecules by coarse-grained molecular dynamics simulations, and revealed the effects of chain length and flexibility on the ordering mechanism [32]. Coarse-grained modeling is convenient for studying the slow ordering processes and universal features of chain molecules, although it omits atomistic details. In our previous study, we considered the attractive interaction between the chain head and substrate. However, the effect of the strength of the attractive force between the whole chain molecule and surface substrate has not been fully investigated. In this study, the ordering dynamics of SAMs are examined by coarse-grained molecular dynamics simulations, specifically focusing on the effects of surface and chain interactions. Our main objective is to clarify the conditions needed to form two-dimensional striped patterns during the initial period of SAM formation of chain molecules from solution. We also examine the adsorption processes of chain molecules to clarify their power law behavior.

II. MODEL

In this study, we carried out coarse-grained molecular dynamics simulations. This model can efficiently describe the slow dynamics of chain molecules by omitting unimportant potential barriers that might markedly slow down the chain dynamics. Although some details might be lost in this coarse-grained approach, this model is effective for understanding the basic physics and universal features of the complicated ordering dynamics of chain molecules.

The model system used here was based on a similar model reported previously [32]. The chain molecules were represented by the worm-like bead-spring model shown in Fig. 1(a). Each chain molecule consisted of a head and a tail.

For the pairwise interaction, we used the Lennard-Jones (LJ) and the soft-core interaction depending on the pair kinds. The LJ potential is given by $U(r) = 4\varepsilon[(\sigma/r)^{12} - (\sigma/r)^{6}]$, and the cutoff distance was 3σ. The LJ potential was used for the interactions between segments that are depicted in the same color in Fig. 1(a): tail and tail segment, solvent and tail segment, solvent and solvent, and head and head segment. The soft-core interaction is given by $U(r) = 4\varepsilon[(\sigma/r)^{12} - (\sigma/r)^{6}] + \varepsilon$, and the cutoff distance was $2^{1/6}\sigma$. The soft-core potential was used for the pair interactions between segments that are marked in different colors in Fig. 1(a): head and tail segment, and solvent and head segment. In this study, the

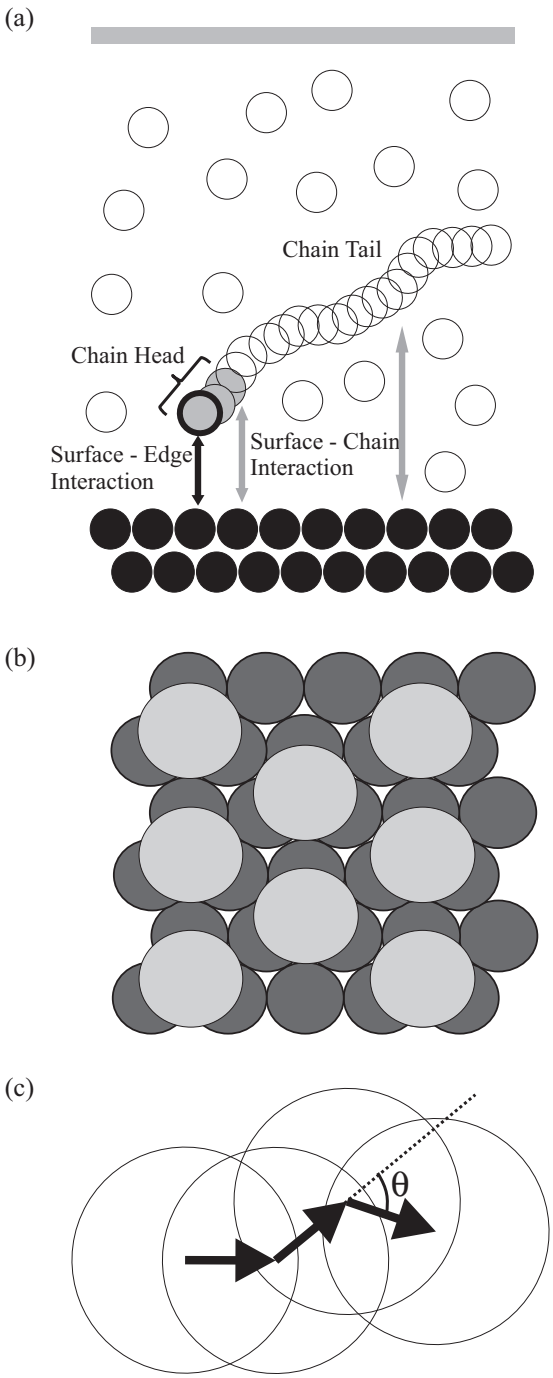

FIG. 1. Schematic diagrams of the simulation model. (a) Molecules in the simulation box. (b) Top view of substrate and chain heads in which the chain molecules are fully packed. Dark and light gray circles indicate substrate atoms and chain heads, respectively. (c) Model of worm-like chain molecules, bond vectors, and bending angle.

model parameters and simulation results have been expressed in dimensionless reduced units, where the segment diameter σ, the energy parameter ε of the LJ interaction potential of chain segments, and the segment mass m were all 1.0. Bonded neighbors and neighbors separated by two bonds in the same chain molecule were excluded in the pairwise calculations.

The bottom of the simulation cells consisted of four layers of (111) surface substrate. The diameter of each surface atom was 0.74. The atom positions of the bottom layer were fixed, and those of the upper three layers were connected by a harmonic potential with a force constant of 20 000. A strong attractive force was applied between the surface and chain edge, which is shown by a gray circle with a black thick line in Fig. 1(a). This surface-edge interaction is given by $U(r) = D[1 - e^{-a(r-r_e)}]^2 - D$, where here $D = 100$, $a = 5.0$, and $r_e = 0.75$. The cutoff distance of the interaction was 3.0. Although this study focused on universal properties and not specific materials, this surface-edge interaction usually corresponds to S-Au bonding in alkanethiol-gold systems. Thus, the strength of this interaction was chosen to be near the same range as follows. The adsorption energy between alkanethiol and gold surface is in the range of 2.4–3.9 $\times$ 10^{-19} J [37–39]. Because the unit of the reduced energy is roughly in the order of 10^{-21} J, we assumed that $D = 100$. A top view of the substrate and fully adsorbed chain heads is illustrated in Fig. 1(b).

The LJ potential was used for the interactions between the substrate surface and chain segments except for the edge of the chain head [gray arrows in Fig. 1(a)]. We changed the strength of this surface LJ potential ε_S between 0.1 and 6.0. We used the value of ε_S as an index to characterize the affinity of the chain for the surface. When the value of ε_S was larger than 1.0, the interaction between a surface atom and chain segment became larger than that between two chain segments.

To confine the solvent and chain molecules to the simulation box, a repulsive wall was included at the top of the simulation box. The potential of this wall is given by $U(r) = 4\varepsilon[\frac{1}{5}(\frac{\sigma}{r})^{10} - \frac{1}{2}(\frac{\sigma}{r})^4 + 0.3]$, in which the cutoff distance of the interaction was 1.0.

In this coarse-grained model, the segments of chain molecules were connected by the harmonic potential given by $U(b) = \frac{1}{2}K_c(b - b_0)^2$, where b_0 is the equilibrium bond length (0.4) and K_c is the elastic constant of the bond springs (9000). The chain rigidity is given by $U(\theta) = \frac{1}{2}K_b(\cos\theta - \cos\theta_0)^2$, in which θ is the angle between two successive bond vectors [Fig. 1(c)] and K_b is the force constant. The equilibrium angle θ_0 was 0. K_b was 4000, which corresponds to the semirigid condition.

Each chain contained 20 units, with three head segments and 17 tail segments. Because the edge segment of each chain overlapped with its bonded neighbor and the neighbor separated by two bonds, the number of head segments, which are shown as gray circles in Fig. 1(a), was three. The number of chain molecules in the system was 320. The number of solvent molecules in the system was 23 200. The size of the simulation box was 19.98 along the x axis, 20.507 along the y axis, and 90.0 along the z axis. The number of molecules and the size of box are the same as the previous study [32]. The box size of the x-y plane was determined so as to fit the periodic structure of the (111) plane of the substrate. Periodic boundary conditions were applied in the horizontal directions (along the x and y axes). Simulations were carried out using an NVT ensemble in which the temperature was 13.0 and the mass of the thermostat was 30 000. The equations of motion were integrated using a fourth-order predictor-corrector method with a time step of 0.001 [40,41]. Simulation results were obtained by averaging

the results for four samples starting from different initial states. These initial states were created independently using random numbers.

To analyze the chain-ordering behavior on the surface of the substrate, we calculated the surface coverage and oriented domain ratio [32,42,43]. The chains adsorbed on the surface were those in which the edge of the chain head was in direct contact with the surface of the substrate. The adsorbed chains have been classified into two types as follows. As shown in Fig. 2(a), if more than half of the chain segments are adsorbed on the surface, the molecules are referred to as "lying" chains. When less than half of the chain segments are adsorbed on the surface, the adsorbed molecules are referred to as "upright" chains. The surface coverage was calculated as the ratio of adsorbed chain molecules to the maximum adsorption number in the simulation area. The maximum adsorption number corresponds to full coverage, in which the alignment of fully packed chain heads is schematically illustrated as gray circles in Fig. 1(b).

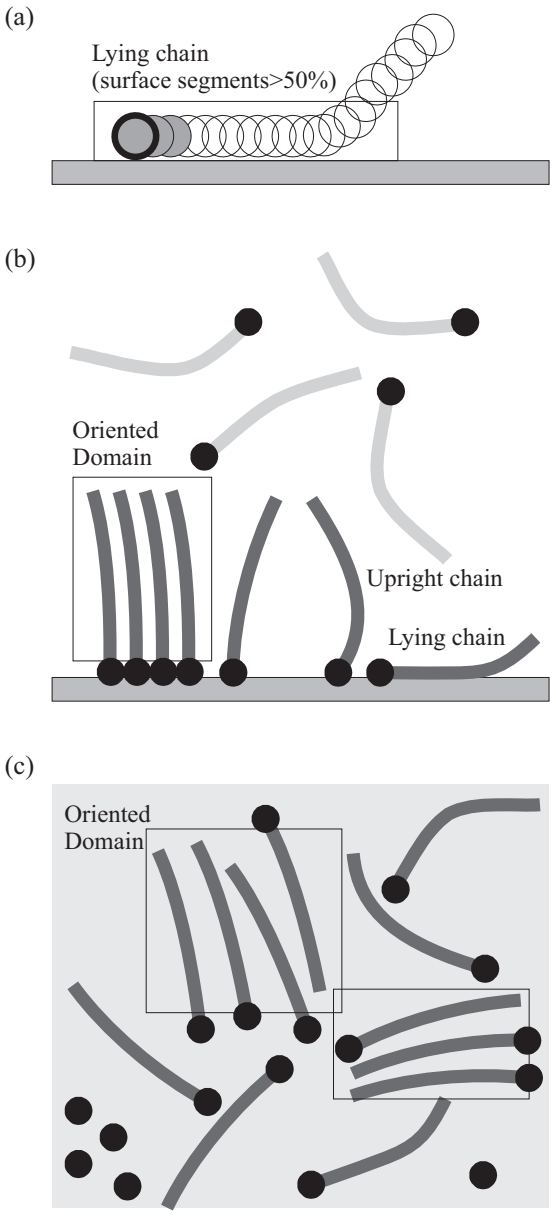

FIG. 2. Schematic diagrams of adsorbed chains on the surface. (a) Example of lying chains. Chains are classified into either upright or lying chains. (b) Example of an oriented domain of upright chains. Oriented domain is the region where the adsorbed chains form an aligned structure. (c) Example of oriented domains of lying chains. For simplicity, only the segments in the vicinity of the surface are shown. In the case of lying structures, the direction of lying chains could vary between domains, especially when the surface is sparsely covered by chains.

An oriented domain is an aligned region of adsorbed chains. Examples of oriented domains are highlighted by rectangles for domains of upright chains in Fig. 2(b) and lying chains in Fig. 2(c). An oriented domain was defined as a large cluster of aligned chain segments whose bond vectors were within a distance of 1.5 of each other and whose difference in orientation was less than 10°. Small aligned groups of less than 50 segments were not included in the oriented domains. The oriented domain ratio was calculated as the ratio of the segment number belonging to oriented domains to the number of fully packed segments on the surface.

We also calculated the global orientation order parameters of the lying chain molecules. An orientation order parameter is given by $\langle 3\cos^2\phi - 1\rangle/2$, in which ϕ is the angle between two bond vectors, which was obtained by averaging over all

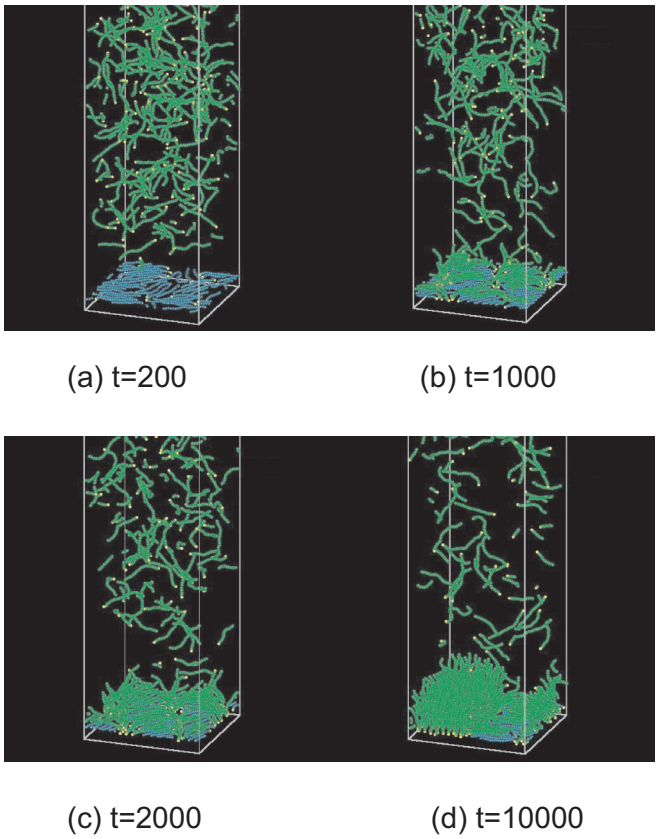

FIG. 3. (Color online) Snapshots of the structure formation processes of chain molecules for strong surface–chain interactions ($\varepsilon_S = 5.0$). Time is shown in dimensionless reduced units. The size of box in the horizontal direction is 19.98 in reduced units. The blue (dark gray) molecules indicate lying chains.

bond vector pairs in the lying chains of the entire system. The orientation order parameter is useful to estimate the development of two-dimensional alignment.

III. RESULTS AND DISCUSSION

First, we discuss a typical example of the ordering process. Snapshots of the formation of ordered structure under the condition of strong surface–chain interactions ($\varepsilon_S = 5.0$) are shown in Fig. 3. In this system, the adsorbed chain molecules initially lie on the substrate surface. As the number of adsorbed chain molecules increases, some chain molecules adopt an upright state. The chain molecules in this upright state form three-dimensionally aligned oriented domains in the intermediate or late period.

We investigated the diffusion and assembly processes of the chain molecules in the vicinity of a surface under various strengths of surface–chain interaction. Figure 4 presents the simulation results obtained for moderate surface–chain interactions of $\varepsilon_S = 1.0$. Here, red (black squares), blue (black circles), and green (light gray circles) symbols indicate the chain head segments, segments of chain molecules lying on the surface, and upright chain segments, respectively. Figures 4(b) and 4(c) reveal that there were many upright chain molecules during the initial period. The random coexistence of lying and upright chain molecules suppressed the formation of oriented domains because they were obstacles for the cohesion of chain molecules. In the intermediate period, the lying chains reoriented and gradually merged into small clusters of upright chains. The clusters of upright chains then formed larger island domains, as shown in Figs. 4(e)–4(g). At $t = 10\,000$, lying

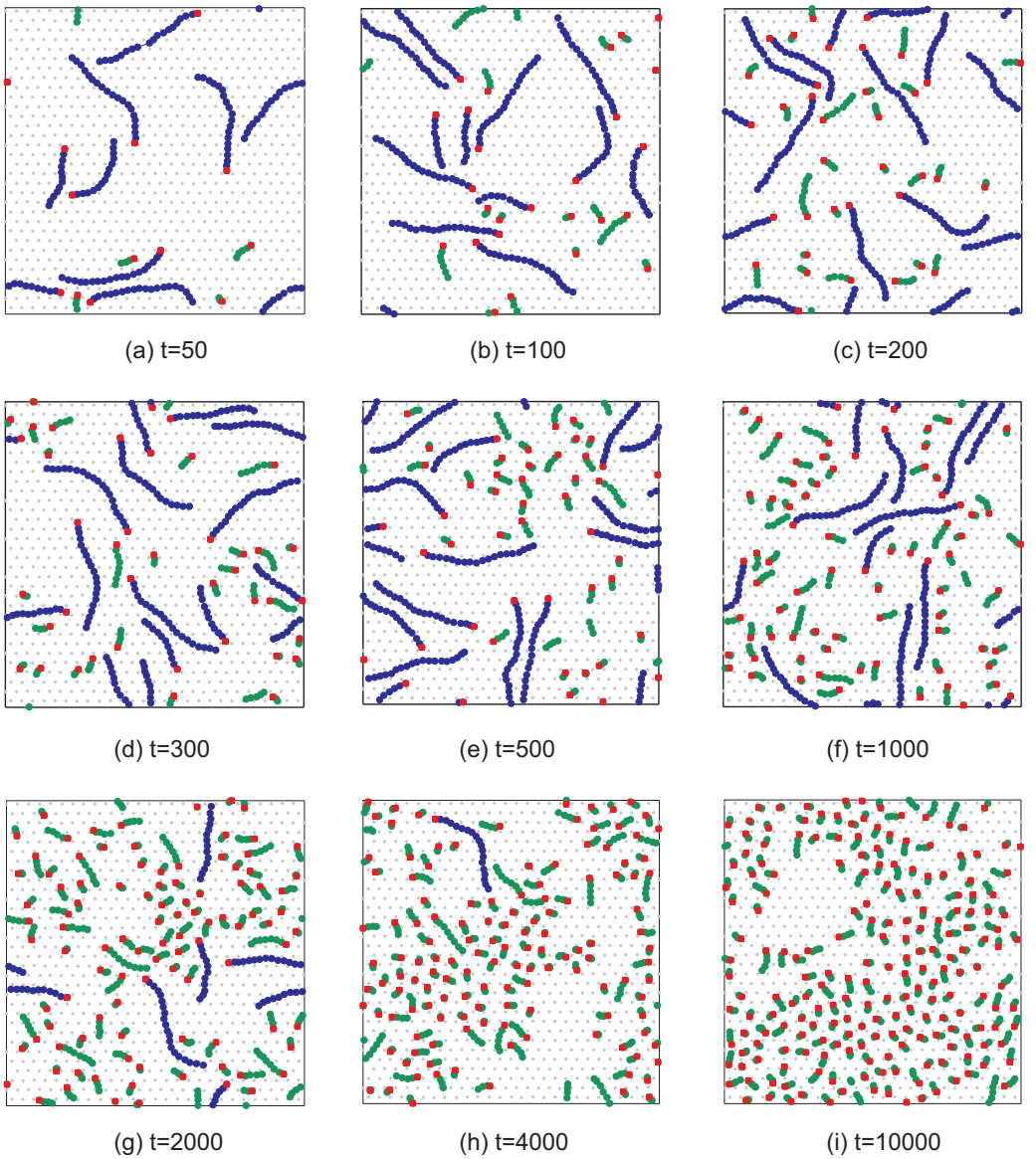

FIG. 4. (Color online) Snapshots of chain configuration on the surface for moderate surface–chain interactions ($\varepsilon_S = 1.0$). The red (black) squares indicate the head segments of chain molecules. The blue (black) circles indicate the segments of lying chain molecules. The green (light gray) circles indicate the surface segments of upright chain molecules. The size of box in the horizontal direction is 19.98 in reduced units. Time is shown in dimensionless reduced units.

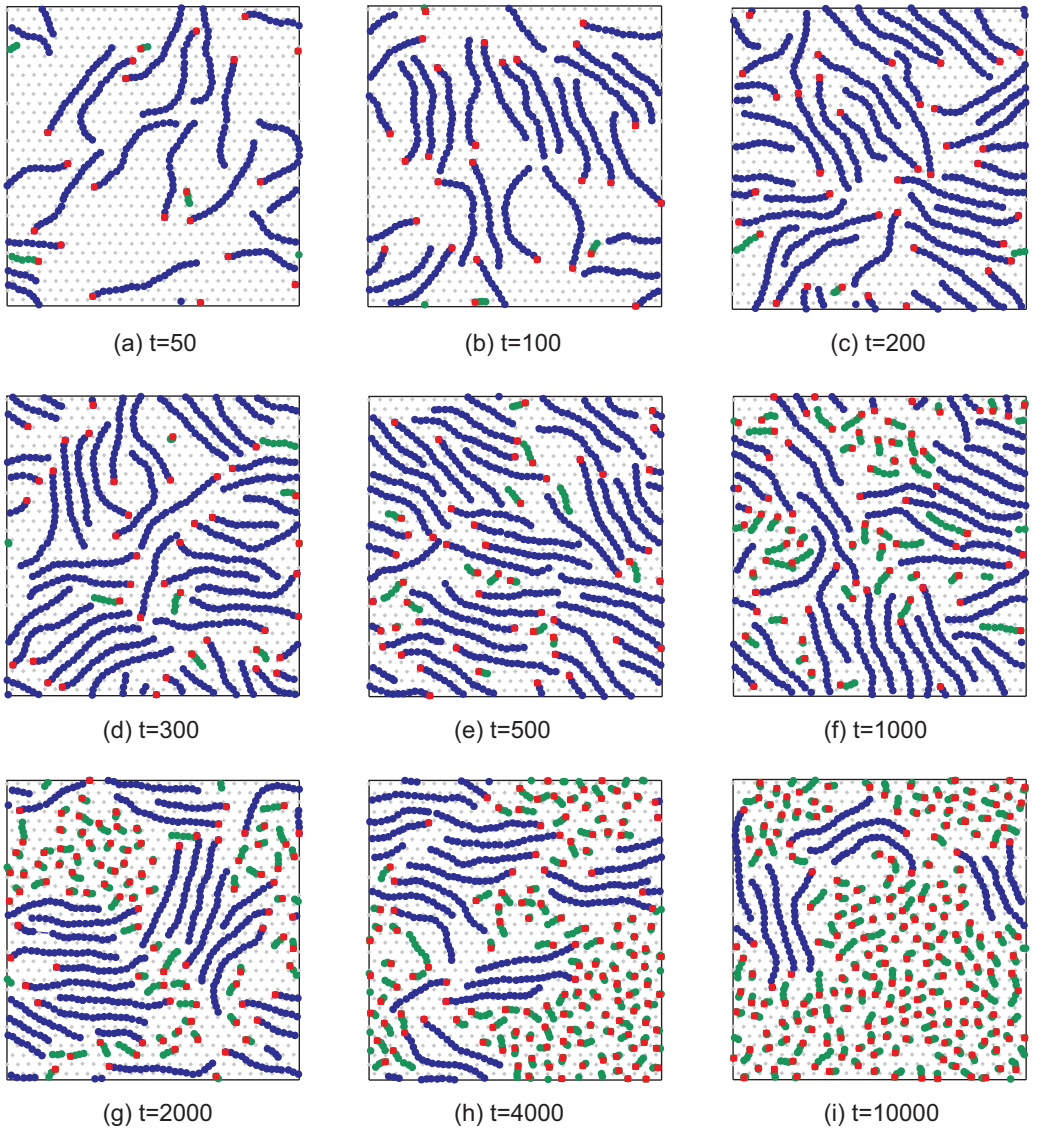

FIG. 5. (Color online) Snapshots of chain configuration on the surface for moderately strong surface–chain interactions ($\varepsilon_S = 2.0$). The symbols and box sizes are the same as described in the caption of Fig. 4.

chains completely disappeared, even though there was enough free surface space for them to remain.

Figure 5 depicts the simulation results obtained for moderately strong surface–chain interactions of $\varepsilon_S = 2.0$. In the initial period before $t = 300$, most of the chain molecules were lying on the surface. However, the development of global alignment of lying chains was slow, and many small clusters formed. At $t = 500$, the surface was mostly covered by chain molecules and large domains with the same chain orientation were observed. In this case, the striped patterns of lying chains were not clearly seen. At $t = 1000$, small clusters of upright chain molecules appeared in the vacant spaces between the lying chain clusters. Then, domains of upright chains grew slowly and eventually covered a large part of the surface area.

The structures of chain molecules adsorbed on the surface under the condition of strong surface–chain interactions ($\varepsilon_S = 5.0$) are shown in Fig. 6. Initially ($t = 50, 100$), the chain molecules formed small clusters on the surface. As chain adsorption proceeded, the lying chains aligned in the same direction, and striped patterns of lying chains were clearly observed between $t = 300$ and 1000. Then, some chain molecules began to stand up near the boundaries of the striped patterns. These upright chain molecules became nuclei for the formation of upright domains that grew slowly in the late period. These results also suggested that the fraction of lying sites increases as the strength of the surface–chain interaction is increased.

Next we show the time evolution of surface coverage. Figures 7(a) and 7(b) illustrate the simulation results for moderate surface–chain interactions of $\varepsilon_S = 1.0$. The dashed line indicates the total surface coverage, while the blue (black) and red (light gray) lines represent the surface coverage of lying and upright chains, respectively. In this case, the strength of the surface–chain interactions is comparable to that of the chain–solvent interactions, which resulted in the initial formation of almost the same amounts of lying and upright

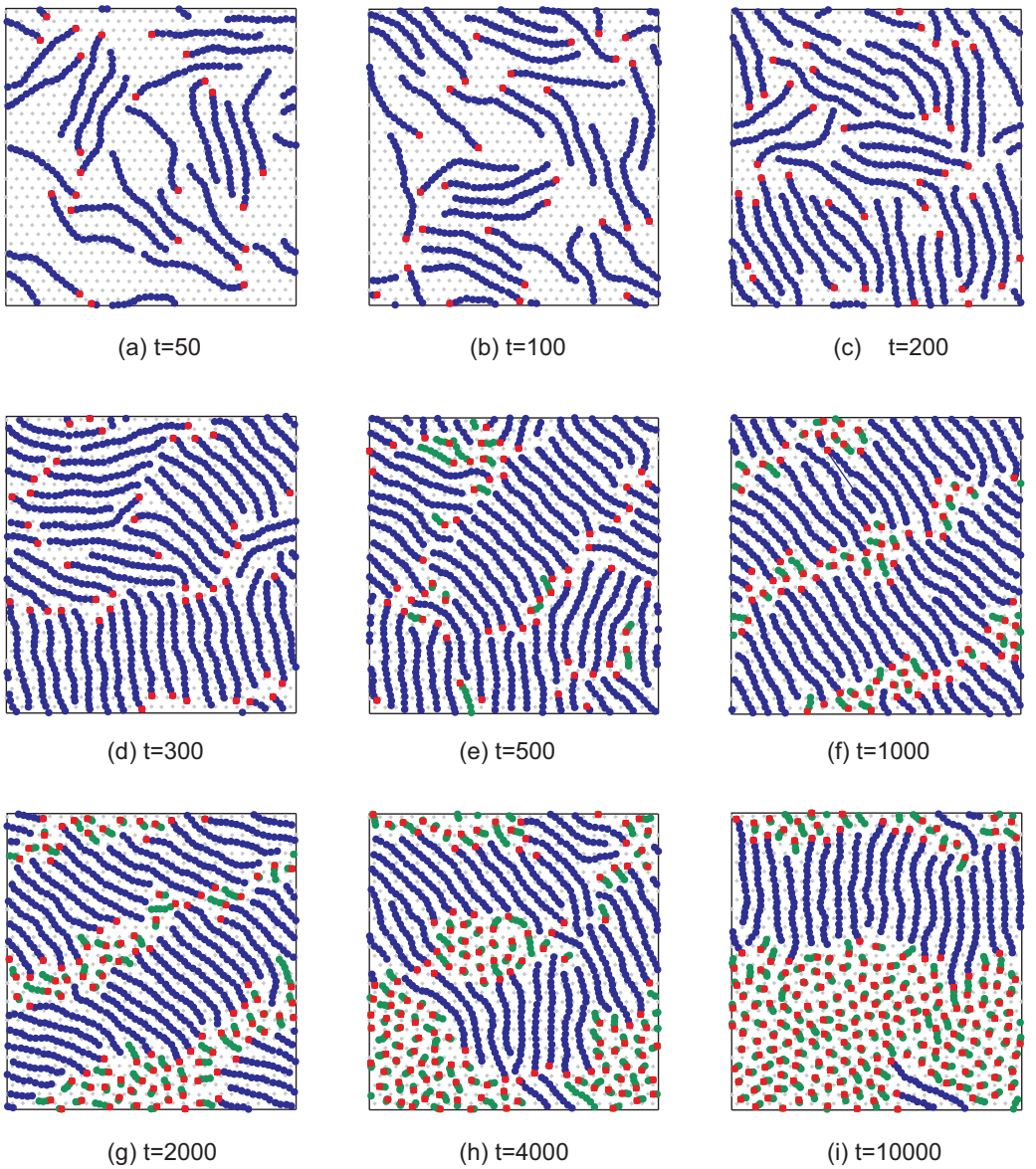

FIG. 6. (Color online) Snapshots of chain configuration on the surface for strong surface–chain interactions ($\varepsilon_S = 5.0$). The symbols and box sizes are the same as described in the caption of Fig. 4. During the intermediate period between $t = 1000$ and 2000, a striped pattern was observed. The domains of upright chains appear in the boundary region of striped patterns in the late period.

chains. However, as the adsorption proceeded, the proportion of lying chains became negligible. Figure 7(b) reveals that the number of chain segments adsorbed on the surface did not reach saturated values and gradually increased in the late period.

Figures 7(c) and 7(d) show simulation results for the evolution of surface coverage under moderately strong surface–chain interactions ($\varepsilon_S = 2.0$). The adsorption and ordering behaviors were largely different from those obtained for moderate surface–chain interactions. Figure 7(c) indicates that the adsorbed chains almost completely adopted a lying structure, and the proportion of upright chains was very small initially. The total number of chain segments adsorbed on the surface was almost saturated after $t = 500$ [Fig. 7(d)]. The rapid growth of upright chains began after $t = 300$ in which the surface had not reached saturation.

Figure 7(e) illustrates the simulation results obtained under the condition of strong surface–chain interactions ($\varepsilon_S = 5.0$). In this case, the qualitative surface-adsorption behavior is similar to that for moderately strong surface–chain interactions. However, when $\varepsilon_S = 5.0$, the adsorbed chains mostly adopted a lying structure until $t = 400$, and an induction time for the development of upright chain molecules was clearly observed. After the induction period, the proportion of upright chains gradually increased. We show the time evolution of the total number of chain segments that are adsorbed on the surface in Fig. 7(f). The number of segments increased rapidly in the initial period, but was almost saturated after $t = 400$. In the late period, upright chain clusters developed from the boundaries of striped patterns on the surface. These observations indicate that upright chains were formed by exclusion of excess chains from the substrate surface.

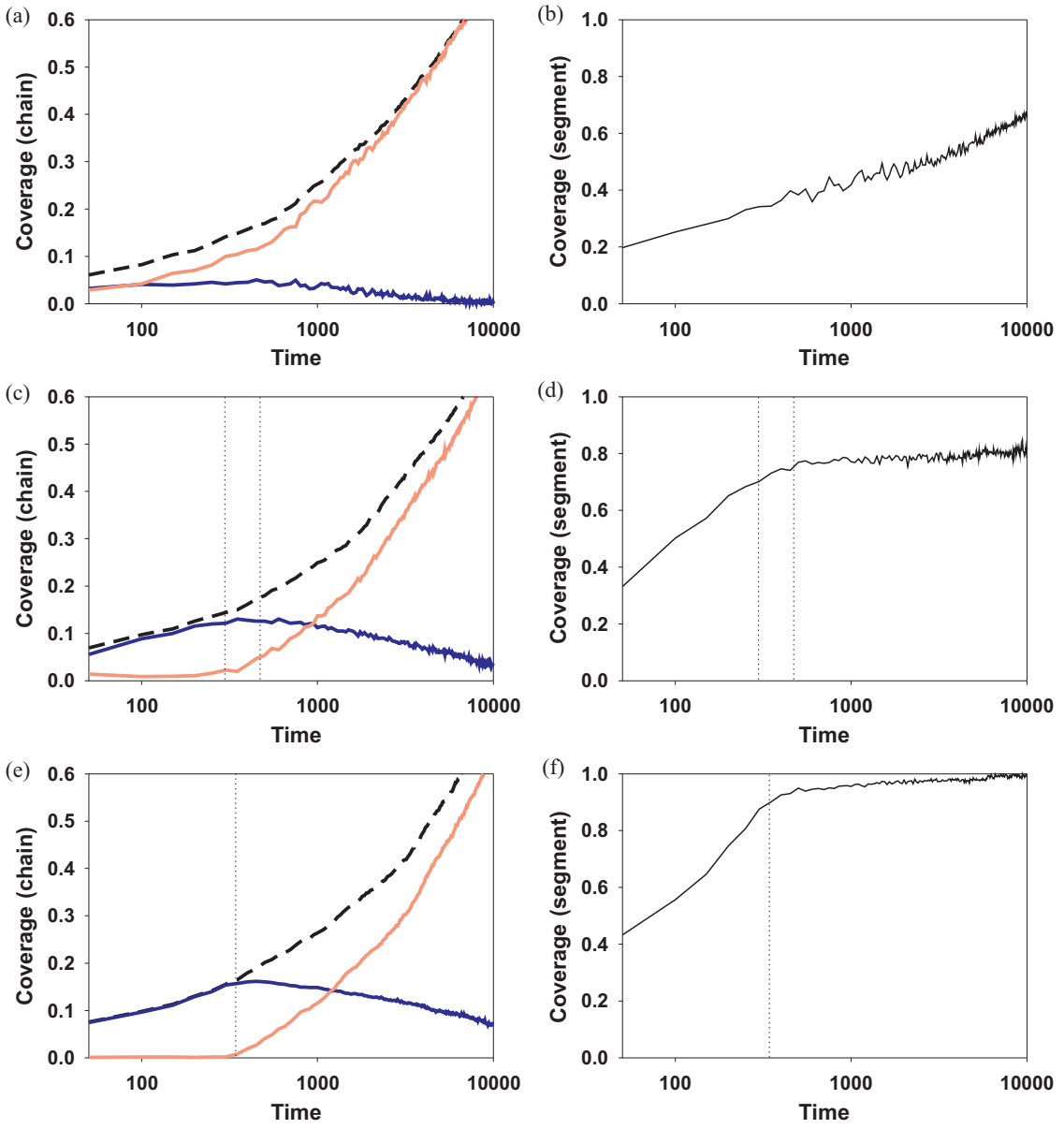

FIG. 7. (Color online) Time evolution of surface coverage for (a) and (b) moderate surface–chain interactions ($\varepsilon_S = 1.0$), (c) and (d) moderately strong surface–chain interactions ($\varepsilon_S = 2.0$), and (e) and (f) strong surface chain–interactions ($\varepsilon_S = 5.0$). In (a), (c), and (d), coverage ratio was calculated from the number of adsorbed chains. The blue (black) and red (light gray) lines indicate the surface coverage of lying and upright chains, respectively. In (b), (d), and (f), coverage ratio was calculated using the number of chain segments in the vicinity of the surface. Dashed vertical lines in (c) and (d) indicate the start of growth of upright chains ($t \sim 300$) and the time at which the growth curve of (d) becomes saturated ($t \sim 500$). Dashed vertical lines in (e) and (f) indicate the start of growth of upright chains ($t \sim 400$).

We have examined the effect of the threshold to distinguish between lying and upright chains. Figure 8 shows the evolution of surface coverage for the moderate surface–chain interactions ($\varepsilon_s = 1.0$). In Fig. 8(a), chains are referred to as lying chains when more than 70% of the segments are adsorbed on the surface. In Fig. 8(b), this threshold is 30%. There are slight differences between the results of high threshold (70%) and those of low threshold (30%). However, these differences would not significantly affect the basic ordering behaviors. Figure 9 shows the evolution of surface coverage for the strong surface–chain interactions ($\varepsilon_S = 5.0$). These results suggested that the transitions between lying and upright chains were relatively sharp and the effect of the threshold was very limited.

The time evolution of the oriented domain ratio under the condition of moderately strong surface–chain interactions ($\varepsilon_S = 2.0$) is presented in Fig. 10(a). The dashed line indicates the total domain ratio, while the blue (black) and red (light gray) lines represent the domain ratios of lying and upright domains, respectively. When $\varepsilon_S = 2.0$, the formation of oriented domains in the initial period was not clearly observed. At $t = 500$, slight development of lying oriented domains was observed, but their content decreased soon afterwards. After a long induction period, upright oriented domains began to

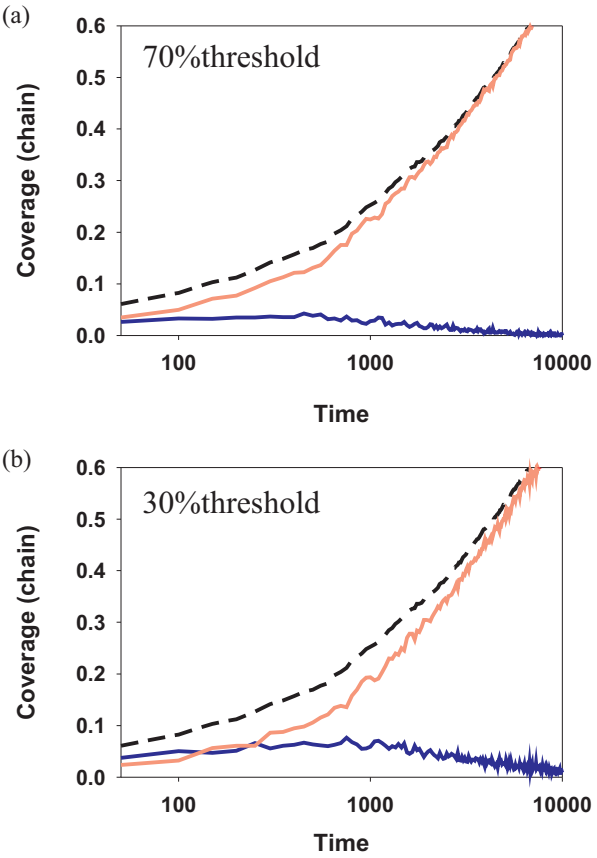

FIG. 8. (Color online) Effect of threshold for moderate surface–chain interactions ($\varepsilon_S = 1.0$). The lines are the same as in Fig. 7.

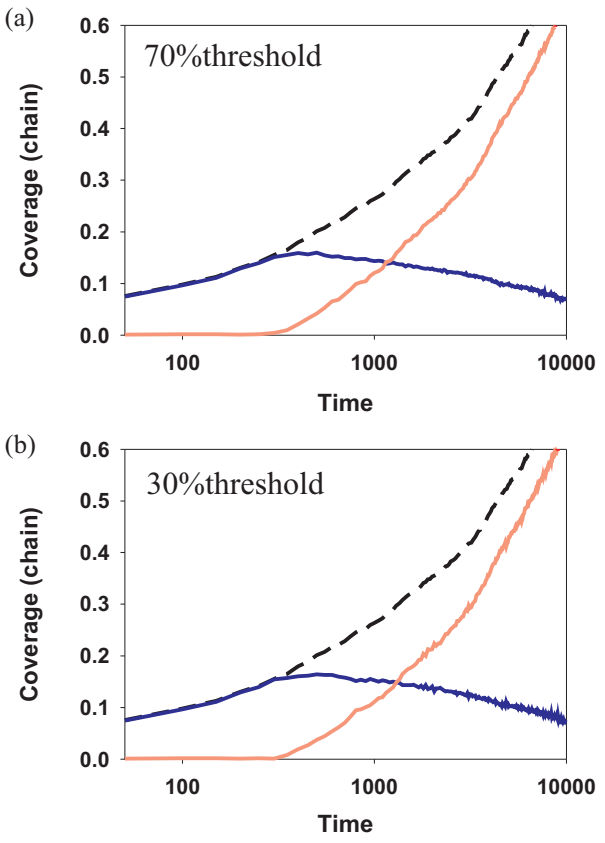

FIG. 9. (Color online) Effect of threshold for strong surface–chain interactions ($\varepsilon_S = 5.0$). The lines are the same as in Fig. 7.

develop from around $t = 1500$. This slow growth of oriented domains may result from the existence of scattered lying chains in the initial or intermediate periods, which became obstacles to the assembly of upright chains. In the meantime, the scattered upright chains were obstacles limiting the assembly of lying chains to form striped patterns.

Figure 10(b) shows the time evolution of the oriented domain ratio under the condition of strong surface–chain interactions ($\varepsilon_S = 5.0$). After their initial fast formation, the proportion of lying oriented domains showed a very slow linear decrease over time. Meanwhile, the content of upright oriented domains showed a slow linear increase after $t = 1000$. The initial growth of upright chain domains was slower than that of the number of upright chains [see Fig. 7 (e)]. Because the upright chains emerge from the narrow area between the striped boundaries and formation of oriented domains requires an assembly process that removes the striped patterns, the formation of upright chain domains is slow.

To characterize the development of striped patterns, we calculated the global orientation orders of lying chain molecules under the condition of strong surface–chain interactions ($\varepsilon_S = 5.0$) in Fig. 11. The global orientation order is an effective index to evaluate the alignment of lying domains, because it approaches 1 when all lying chain molecules align in the same direction and form a complete striped pattern. Note that the global orientation order approaches 0 when the direction of lying chains varies randomly between domains, even if the directions of lying chains within a single domain align completely in the same direction. Figure 11 reveals that the two-dimensional global orientation order rapidly increased until $t = 1000$, then gradually increased with large fluctuation in the late periods. The rapid growth of the global orientation order between $t = 400$ and 1000 reflected the development of the striped pattern on the surface. There was a large fluctuation of orientation order after $t = 1000$. When parts of the striped patterns were destroyed in the late period [e.g., Fig. 6(h)], the direction of orientation of the disappearing region changed considerably. In contrast, if the area of the striped region decreased, the global orientation order could improve because there is no need to average over many oriented domains that might have assumed slightly different directions to each other.

The relationship between the strength of the surface–chain interaction and the formation of lying structures is summarized in Fig. 12. Figure 12(a) plots the maximum values of the surface coverage ratio of lying chains during the ordering process. For weak surface–chain interactions ($\varepsilon_S < 2$), the content of lying chains increased with the surface–chain interaction. In this case, the number of lying chains is small, and lying chains cannot form oriented domains, as indicated in Fig. 12(b). Lying domains are clearly observed when the strength of the surface–chain interactions is 2 or higher. This threshold may be roughly explained as a result of competition between assembly processes. When the strength of the surface–chain interactions is of the same order as that

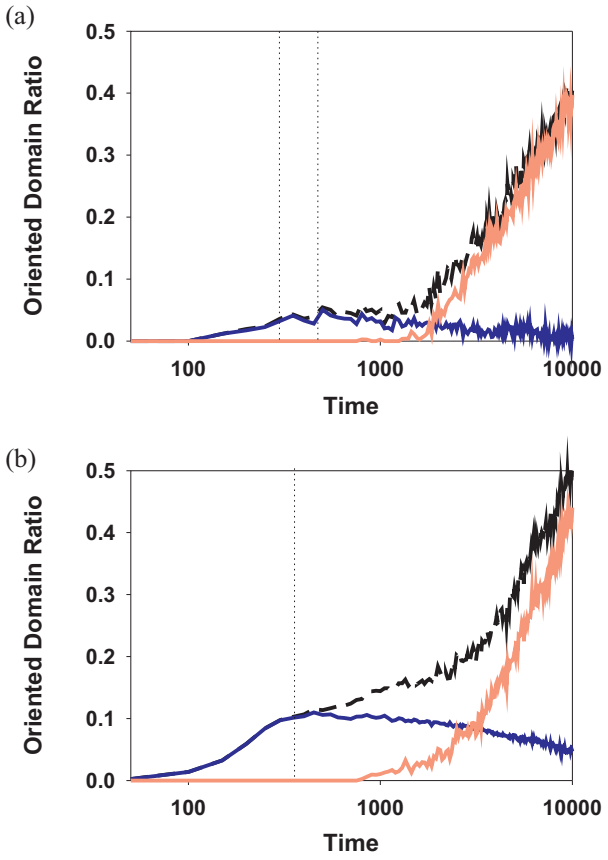

FIG. 10. (Color online) Time evolution of oriented domain ratio for (a) moderately strong surface–chain interactions ($\varepsilon_S = 2.0$), and (b) strong surface–chain interactions ($\varepsilon_S = 5.0$). The blue (black) and red (light gray) lines indicate domains of lying and upright chains, respectively. The dashed thick line indicates the overall domain ratio. For comparison of time evolution, the dashed vertical lines in Fig. 7 are also shown in this figure.

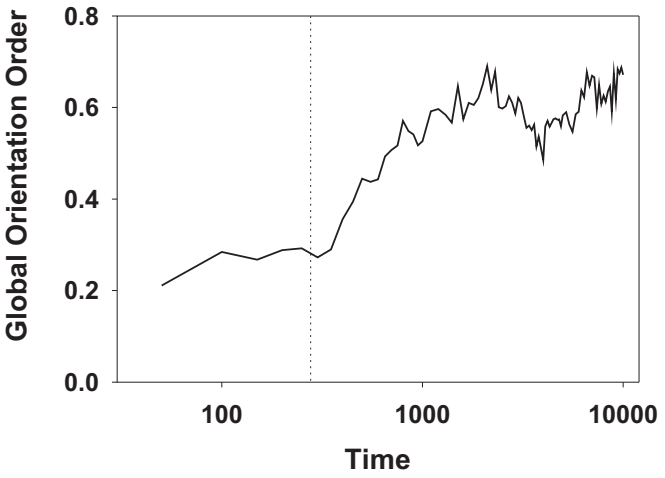

FIG. 11. Time evolution of the global orientation order parameter of lying chains for strong surface–chain interactions ($\varepsilon_S = 5.0$). For comparison of time evolution, the dashed vertical line in Fig. 7 is also shown in this figure. The rapid growth of the order parameter between $t = 400$ and 1000 reflects the development of a striped pattern on the surface.

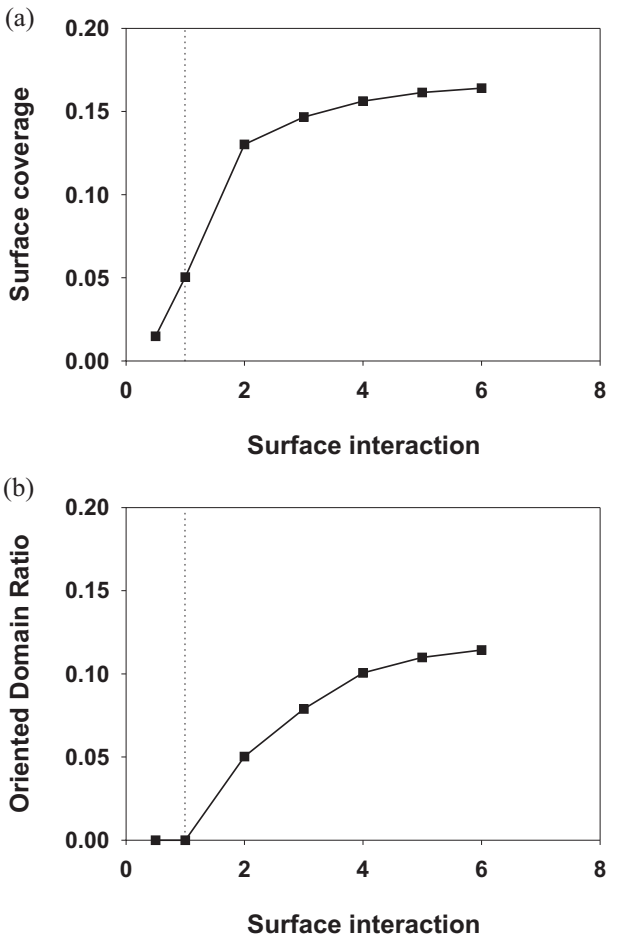

FIG. 12. Dependence of surface-chain interaction on the formation of oriented domains of lying chains. (a) Maximum surface coverage of lying chains in the structure formation processes. (b) Maximum oriented domain ratio of lying chains in the structure formation processes.

of the chain–chain interactions, the chains lying on the surface can easily stand and assemble with each other. However, if the surface–chain interactions are twice as strong as the chain–chain interactions, nuclei formed of only two upright chains are unstable. The simultaneous assembly of many chains is required for nucleation of upright chain clusters. This makes the probability of formation of such nuclei extremely low, and the lying domains readily grow. In the case of strong surface–chain interactions ($\varepsilon_S = 5.0$), an upright domain is only formed when the free surface area is not sufficient for further growth of lying domains.

In Fig. 13, we compare the adsorption processes of chain heads with different degrees of surface–chain interaction. There was small increase in the surface coverage for systems with stronger surface–chain interactions at the beginning. However, overall behaviors are similar and the growth curve of total surface coverage can be expressed by the power law $\sigma = At^{\nu}$. In the case of strong surface–chain interactions ($\varepsilon_S = 5.0$), A is 0.016 and ν is 0.41. This curve is similar to the growth curve of diffusion-limited adsorption, which is expressed by $\sigma = At^{0.5}$. Although the ordering behavior of

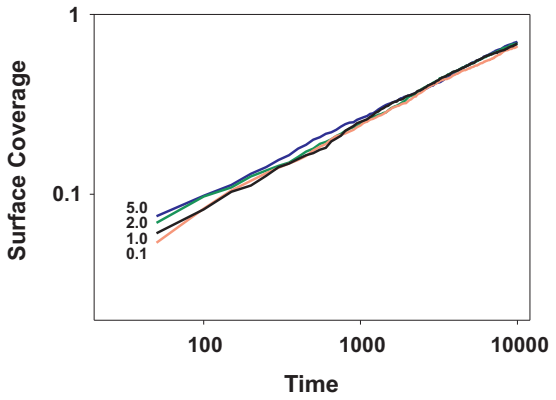

FIG. 13. (Color online) Adsorption curves for different surface-chain interactions ($\varepsilon_S = 0.1, 1.0, 2.0, 5.0$). Time evolution curves of surface coverage can be expressed by power laws.

chain molecules on the surface was strongly influenced by the strength of surface–chain interactions, the adsorption curves of the chain molecules did not show such large differences. Adsorption processes are mainly governed by the diffusion of chain molecules in the solution, and it turned out that the formation of a thin adsorbed structure does not have large influence on ordering behavior.

We considered theoretically the adsorption kinetics of chain molecules in aqueous phase by diffusion. The concentration of chain molecules at a distance x away from the adsorption surface is assumed to be homogeneous in any plane parallel to the substrate. Then, the concentration $c(x,t)$ of chain molecules in the aqueous phase obeys the diffusion equation,

$$\frac{\partial}{\partial t}c(x,t) = D\frac{\partial^2}{\partial x^2}c(x,t), \tag{1}$$

where D denotes the diffusion coefficient. We denote the number of lying chains on the surface as $\Gamma_1(t)$ and the number by upright chains on the surface as $\Gamma_2(t)$. The ratio of the surface occupied by upright chains to that occupied by lying chains is denoted γ_{12}. The surface coverage of lying chains satisfies the *Langmuir* adsorption equation,

$$\frac{\partial}{\partial t}\Gamma_1(t) = k_a c(0,t)[\Gamma_m - \Gamma_1(t) - \gamma_{12}\Gamma_2(t)] - k_2\Gamma_1(t)^2, \tag{2}$$

where k_a is the adsorption rate, Γ_m is the maximum surface coverage, and k_2 is the rate that the lying chains change into upright chains. We assume that upright chains are generated by interactions between lying chains as follows:

$$\frac{\partial}{\partial t}\Gamma_2(t) = k_2\Gamma_1(t)^2. \tag{3}$$

The initial condition is $c(x,0) = c_0$. The total number of chain molecules given by $\Gamma(t) = \Gamma_1(t) + \Gamma_2(t)$ satisfies the boundary condition at the surface expressed by the continuity equation,

$$\frac{\partial}{\partial t}\Gamma(t) = D\frac{\partial}{\partial x}c(x,t)|_{x=0}, \tag{4}$$

and another boundary condition is $\lim_{x\to\infty} c(x,t) = c_0$.

By eliminating $c(x,t)$ in Eqs. (1) and (2), we obtain [44–46]

$$\frac{\partial}{\partial t}\Gamma_1(t) = k_a\left[c_0 - \frac{\partial}{\partial t}\int_0^t dt_1 \frac{1}{\sqrt{\pi D(t-t_1)}}\Gamma(t_1)\right] \times [\Gamma_m - \Gamma_1(t) - \gamma_{12}\Gamma_2(t)] - k_2\Gamma_1(t)^2. \tag{5}$$

The equation for the total number of adsorbed chain molecules can be obtained by summation of Eqs. (3) and (5), as

$$\frac{\partial}{\partial t}\Gamma(t) = k_a\left[c_0 - \frac{\partial}{\partial t}\int_0^t dt_1 \frac{1}{\sqrt{\pi D(t-t_1)}}\Gamma(t_1)\right] \times [\Gamma_m - \Gamma_1(t) - \gamma_{12}\Gamma_2(t)]. \tag{6}$$

If $\gamma_{12} = 1$, Eq. (6) is equal to the adsorption equation of a single species and the result can be approximately given by [47]

$$\Gamma(t) = 2c_0\sqrt{Dt/\pi}, \tag{7}$$

in the diffusion-controlled limit. Time evolution of the total number of chain molecules can be similar to the usual diffusion-controlled adsorption until the saturation occurs [44].

Next, we solve Eqs. (3) and (5) by introducing dimensionless variables defined as $\theta = \Gamma(t)/\Gamma_m$, $\theta_1 = \Gamma_1(t)/\Gamma_m$, and $\theta_2 = \Gamma_2(t)/\Gamma_m$. The dimensionless time is defined by $(t/D)k_a^2\Gamma_m^2$. The time evolution is calculated by discretizing the dimensionless time by the small interval denoted as h using Euler's method and the Grünwald-Letnikov formula [48,49],

$$\frac{\partial}{\partial t}\int_0^t dt_1 \frac{1}{\sqrt{\pi(t-t_1)}} f(t_1) = \frac{1}{\sqrt{h}}\sum_{j=0}^{[t/h]}\omega_j f(t-jh), \tag{8}$$

where the integer part of t/h is given by $[t/h]$ and ω_j can be obtained from

$$\omega_0 = 1, \quad \omega_k = \left(1 - \frac{4}{2k}\right)\omega_{k-1}. \tag{9}$$

In Fig. 14, we show the surface coverage as a function of dimensionless time for $h = 0.01$. The results were not influenced by the temporal discretization by choosing small values of h. The surface coverage of lying chains exhibits a maximum and decreases after a long time. The surface coverage of upright chains increases slowly. The total number of adsorbed chain molecules increases with time and exhibits the typical diffusion-controlled time evolution given by Eq. (7) until saturation occurs. These results are qualitatively similar to those of molecular dynamics simulations when the interaction between the surface atom and a chain segment is moderately strong ($\varepsilon_s = 2$).

Although the internal conversion from lying to upright chains takes place, the total number of chain molecules exhibits a simple time evolution as if the internal conversion is absent. We have shown theoretically that the total number of adsorbed chain molecules is not affected by their internal conversion, consistent with the results of our molecular dynamics simulations.

The direct observation of ordering processes of SAM is not always easy, but there are some reports of SAM formation involving two steps [7–9]. Our simulation results

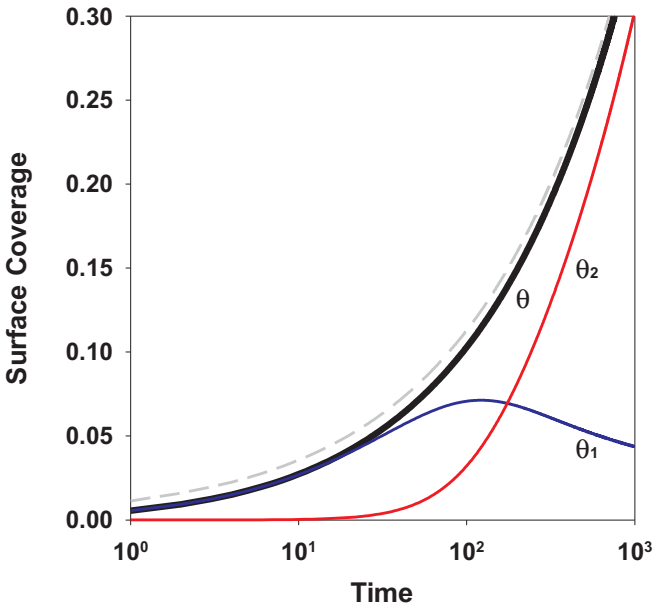

FIG. 14. (Color online) Surface coverage as a function of dimensionless time defined by $(t/D)k_a^2\Gamma_m^2$. Simulation parameters were $Dk_2/(k_a^2\Gamma_m^2) = 0.1$, $Dc_0/(k_a\Gamma_m^2) = 0.01$, and $\gamma_{12} = 0.01$. The thin solid lines represent the surface coverage by lying (θ_1) and upright (θ_2) chains, respectively. The thick solid line denotes the total number of adsorbed chain molecules divided by Γ_m. The long dashed line represents $2c_0\sqrt{Dt/\pi}$, which corresponds to the diffusion-controlled limit.

indicate that the ordering process has two steps when the surface–chain interaction is sufficiently greater than the chain–chain interaction. Two-dimensional ordering occurs when the surface–chain interactions are large ($\varepsilon_S > 2$), as shown in Fig. 12. When the strength of the surface–chain interactions was comparable to or less than that of chain–chain interactions, a two-dimensionally ordered structure was not observed and the adsorbed chains adopted brush-like structures.

The formation of a SAM is a complicated ordering process because of the competition between adsorption, assembly, and surface diffusion. This simulation study systematically changed the surface interactions and revealed the detailed behavior of the ordering dynamics. These simulation results provide us with useful information to help understand the ordering dynamics of chain molecules on surfaces.

IV. CONCLUSION

The effects of surface-chain interactions on the ordering dynamics of SAMs of chain molecules were studied using coarse-grained molecular dynamics simulations to elucidate the detailed mechanisms of formation and dissociation of two-dimensionally ordered structures such as striped patterns.

When the strength of surface–chain interactions is equal to that of chain–chain interactions, the oriented domains of upright chain molecules are formed spontaneously initially, and the ordering proceeds by growth of these island domains. In this case, the ratio of upright to lying chains is comparable in the initial period. The lying chains cannot form nuclei of two-dimensional-oriented domains but easily reorient and merge into the domains of upright chains by fluctuation.

In contrast, when the strength of surface–chain interactions is at least twice that of chain–chain interactions, the adsorbed chains tend to adopt a lying structure initially. These lying chains form two-dimensional-oriented domains in the intermediate period. In the late period, upright chains emerged from the domain boundaries of two-dimensionally aligned structures. In the case of extremely strong surface–chain interactions, domains of upright chains formed only after the surface was mostly covered by chain molecules. This is because the nucleation of upright chain domains requires simultaneous assembly of many chain molecules. In this case, the rearrangement of chain molecules keeping the chains aligned on the surface prevails against the formation of nuclei of the upright structure. This leads to the formation of a striped pattern on the surface.

Although the ordering processes of chain molecules on a surface is strongly influenced by the strength of the surface–chain interactions, the adsorption rate on the surface is less affected by this factor because it is mainly governed by the diffusion of chain molecules in the solution. We analyzed the maximum area of oriented domains of lying chains by solving coupled equations of diffusion and that describing the structure growth on the surface. Although the internal conversion from lying to upright chains was taken into account, the total number of chain molecules adsorbed on the surface exhibits a simple time evolution as if the internal conversion is absent. These calculations support the results of our molecular dynamics simulations that indicate the total number of adsorbed chain molecules is not strongly affected by their internal conversion.

In this study, we investigated the adsorption behavior of semirigid chain molecules. For flexible chain molecules, the ordering processes to form two-dimensional and three-dimensional structures might be slightly different because the flexible chain molecules randomly cover the surface so adsorption and diffusion to the surface are inhibited to some extent. For short-chain molecules, it is expected that the energy barrier to form three-dimensional nuclei will be small, which might lead to a decrease in the amount of the initial two-dimensional structures formed.

Overall, this study revealed that the development of two-dimensionally aligned domains such as striped patterns requires sufficiently strong surface–chain interactions to prevent the spontaneous formation of nuclei of domains of upright chains, while the overall adsorption kinetics are less affected by internal conversion of chain molecules on the surface.

[1] A. Ulman, Chem. Rev. **96**, 1533 (1996).
[2] D. S. Karpovich and G. J. Blanchard, Langmuir **10**, 3315 (1994).
[3] K. Bierbaum, M. Grunze, A. A. Baski, L. F. Chi, W. Schrepp, and H. Fuchs, Langmuir **11**, 2143 (1995).

[4] I. Doudevski, W. A. Hayes, and D. K. Schwartz, Phys. Rev. Lett. **81**, 4927 (1998).
[5] K. A. Peterlinz and R. Georgiadis, Langmuir **12**, 4731 (1996).
[6] O. Dannenberger, M. Buck, and M. Grunze, J. Phys. Chem. B **103**, 2202 (1999).
[7] Y. Han, H. Noguchi, K. Sakaguchi, and K. Uosaki, Langmuir **27**, 11951 (2011).
[8] G. E. Poirier and E. D. Pylant, Science **272**, 1145 (1996).
[9] G. E. Poirier, Langmuir **15**, 1167 (1999).
[10] L. Tang, F. S. Li, and Q. Guo, J. Phys. Chem. C **117**, 21234 (2013).
[11] F. Li, L. Tang, O. Voznyy, J. Gao and Q. Guo, J. Chem. Phys. **138**, 194707 (2013).
[12] Y. Leng, D. J. Keffer, and P. T. Cummings, J. Phys. Chem. B **107**, 11940 (2003).
[13] Y. H. Jang, S. S. Jang, and W. A. Goddard, J. Am. Chem. Soc. **127**, 4959 (2005).
[14] D. M. Duffy and J. H. Harding, Langmuir **21**, 3850 (2005).
[15] R. Pool, P. Schapotschnikow, and T. J. H. Vlugt, J. Phys. Chem. C **111**, 10201 (2007).
[16] O. Alexiadis, K. C. Daoulas, and V. G. Mavrantzas, J. Phys. Chem. B **112**, 1198 (2008).
[17] L. Ferrighi, Y. Pan, H. Gronbeck and B. Hammer, J. Phys. Chem. C **116**, 7374 (2012).
[18] N. Gronbech-Jensen, A. N. Parikh, K. M. Beardmore, and R. C. Desai, Langmuir **19**, 1474 (2003).
[19] A. V. Shevade, J. Zhou, M. T. Zin, and S. Jiang, Langmuir **17**, 7566 (2001).
[20] J. Z. Y. Chen, Phys. Rev. E **82**, 060801 (2010).
[21] S. Karalus, W. Janke, and M. Bachmann, Phys. Rev. E **84**, 031803 (2011).
[22] A. Swetnam, and M. P. Allen, Phys. Rev. E **85**, 062901 (2012).
[23] M. G. Opferman, R. D. Coalson, D. Jasnow, and A. Zilman, Phys. Rev. E **86**, 031806 (2012).
[24] L. I. Klushin, A. A. Polotsky, H. P. Hsu, D. A. Markelov, K. Binder and A. M. Skvortsov, Phys. Rev. E **87**, 022604 (2013).
[25] P. Y. Lai, J. Chem. Phys. **98**, 669 (1993).
[26] R. Zajac and A. Chakrabarti, Phys. Rev. E **49**, 3069 (1994).
[27] R. Zajac and A. Chakrabarti, Phys. Rev. E **52**, 6536 (1995).
[28] A. Kopf, J. Baschnagel, J. Wittmer, and K. Binder, Macromolecules **29**, 1433 (1996).
[29] S. B. Opps, B. Yang, C. G. Gray, and D. E. Sullivan, Phys Rev. E **63**, 041602 (2001).
[30] G. D. Smith, Y. Zhang, F. Yin, D. Bedrov, M. D. Dadmun, and Z. Huang, Langmuir **22**, 664 (2006).
[31] O. Alexiadis, V. G. Mavrantzas, R. Khare, J. Beckers, and A. R. C. Baljon, Macromolecules **41**, 987 (2008).
[32] T. Miura and M. Mikami, Phys. Rev. E **81**, 021801 (2010).
[33] Y. Ahn, J. K. Saha, G. C. Schatz, and J. Jang, J. Phys. Chem. C **115**, 10668 (2011).
[34] G. S. Longo, S. K. Bhattacharya, and S. Scandolo, J. Phys. Chem. C **116**, 14883 (2012).
[35] S. Živković, Z. M. Jakšić, I. Lončarević, Lj. Budinski-Petković, S. B. Vrhovac, and A. Belić, Phys. Rev. E **88**, 052131 (2013).
[36] T. Yi and S. Lichter, Phys. Rev. E **89**, 062404 (2014).
[37] H. Gronbeck, A. Curioni, and W. Andreoni, A. Am. Chem. Soc. **122**, 3839 (2000).
[38] T. Hayashi, Y. Morikawa, and H. Nozoye, J. Chem. Phys. **114**, 7615 (2001).
[39] Y. Yourdshahyan and A. M. Rappe, J. Chem. Phys. **117**, 825 (2002).
[40] D. Frenkel and B. Smit, *Understanding Molecular Simulation* (Academic Press, San Diego, 1996).
[41] D. C. Rapaport, *The Art of Molecular Dynamics Simulation* (Cambridge University Press, Cambridge, 1995).
[42] T. Miura, R. Kishi, and M. Mikami, J. Chem. Phys. **119**, 6354 (2003).
[43] T. Miura and M. Mikami, Phys. Rev. E **75**, 031804 (2007).
[44] A. F. H. Ward and L. Tordai, J. Chem. Phys. **14**, 453 (1946).
[45] K. Seki and M. Tachiya, J. Chem. Phys. **113**, 3441 (2000).
[46] T. Miura and K. Seki [J. Phys. Chem. B (to be published)].
[47] I. Langmuir and V. J. Schaefer, J. Am. Chem. Soc. **59**, 2400 (1937).
[48] S. B. Yuste, and L. Acedo, SIAM J. Numer. Anal. **42**, 1862 (2005).
[49] I. Podlubny, *Fractional Differential Equations* (Academic Press, San Diego, 1999).